

Load Rating and Buckling of Circular Concrete-Filled Steel Tube (CFST): Simulation and Experiment

L H Vu, N C Duc, L V Dong, D L Truong, N M T Anh, H Q Hung and P V Hue

Mien Trung University of Civil Engineering, Ministry of Construction of the Socialist Republic of Vietnam

E-mail: lehoangvu@muce.edu.vn, nguyencongduc@muce.edu.vn

Abstract. The paper studies estimate ultimate strength and local buckling of circular concrete filled steel tube (CFST) specimens subjected to axial load using strain gage, force transducer and displacement sensor. The strain responses of CFST column in testing procedure and the results of finite element modelling will be used to predict failure modes when cracks occur in concrete core and deformation increases on steel tube's surface. Besides, the principles of Eurocode 4 and AISC 360-10 are used to calculate the critical buckling stress in comparison with experimental approach and numerical evaluation. Combining experimental and simulation data can be very useful for diagnostic load rating and limit, and effective to evaluate the damage on structural health monitoring of CFST members.

1. Introduction

It is undeniable that concrete structures with CFST members play a major role in modern construction structures and materials for coastal and island construction buildings in recent years. CFST column using high-strength steel is one of the most promising new developments to increase fatigue life of concrete and reduce corrosive effects of seawater for concrete structures in coastal areas. The behavior of CFST column under compressive axial load is an important factor in limit load analysis for engineers that will be calculated by using finite element method (FEM), can be estimated via testing methods and measurements. The familiar research of this problem is the response of circular and square thin-walled CFST specimens with length-to-diameter ratios subjected to axial loading through finite element analysis (FEA) model to predict bearing capacity and the failure modes, experimental analysis using displacement transducer and strain gauges to plot load versus strain curve [2].

In addition, Investigating failure under flexural buckling of CFST columns by an experimental study was compared with compression load limits in the South African code (SANS 10162-1) and Eurocode 4 (EC4) [3]. Experimental behavior of circular CFST columns with different L/D ratios and D/t ratios are based on EC4 and AISC 360-10 predictions [4]. Also, Experimental investigations with displacement transducers using the Design of Experiments (DOE) approach on circular CFT samples with D/t ratio of 22.3-50.8 and L/D ratio of 7.8-22.5, were compared with AISC-LRFD-2005 and EC4-1994 [1].

Besides, there are many studies for experimental approaches and some other papers only focus on theoretical methods: Computer-aided engineering (CAE) and Design Codes. To illustrate, new theoretical model developed to analyze the axial and lateral stress-strain response of CFT columns by integrating a lateral-to-axial strain model of confined concrete, an axial stress-strain model of confined concrete, and a biaxial stress-strain model of steel tube [5]. A parametric study was investigated on the effects of concrete strength, steel pile, FRP wraps and steel ring properties on the structural capabilities of external CFST columns [6]. The F.E modelling of confined concrete and steel



tube (concrete-steel interface) was analyzed and compared with CFST specimens tested by other published researches [7].

Similarly, the behavior of concrete-encased CFST columns, concrete-encased CFST, hollow RC and conventional CFST with square and circular section under combined compression and torsion were investigated according to the Chinese design guideline for concrete structures GB50010-2010, experimental method using strain gages to predict shear strain and failure modes [8]. Axial compressive strength and ductility of CFST stub columns using new approach for reducing the axial stress in the steel tube were experimentally studied [9]. Tensile properties of steel in CFST columns applied to a cyclic loading and corrosion test [10].

There has been no shortage of heated discussion on the issues from experiment to computation, and the purpose of the present works was to study the behavior of CFST specimens under axial load. The specimens were analyzed theoretically and experimentally to estimate the capacity of CFST and to calculate ultimate compressive strength, and determine positions of local buckling through the 3D-finite element modelling of steel tube and concrete core, together with testing procedures via measuring strain, displacement and force.

2. Experimental investigation and computational model evaluation

An overall view of the test facilities in the experimental study will be as shown in Figure 1 and 2. The system consists of stand-alone Mobile Base Station along and three four-channel Nodes, which can communicate through wireless with the user's PC. WinSTS software controls over the wireless structural testing system (STS-WiFi) to monitor Node status, signal strength, and record sensor signals. The wireless structural testing system was supplied by Bridge Diagnostics - USA [17].

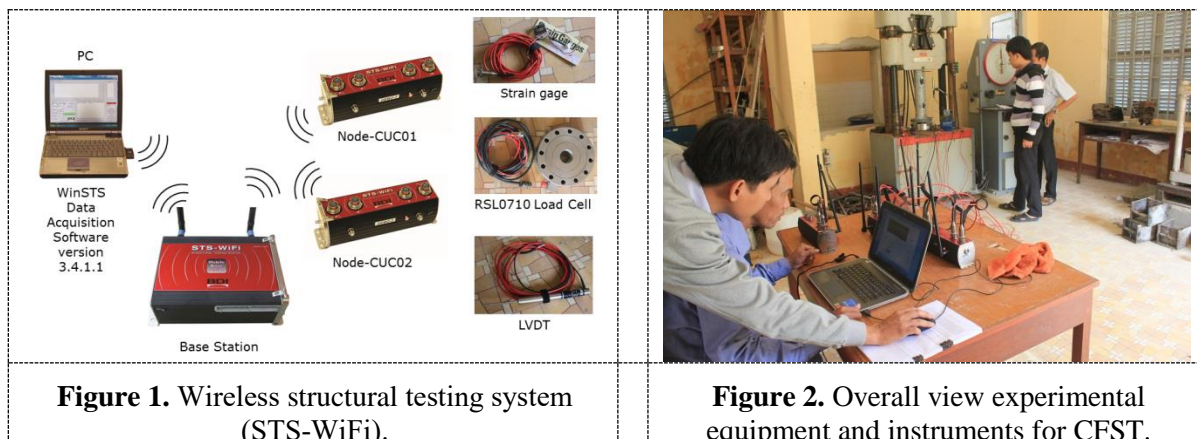


Figure 1. Wireless structural testing system (STS-WiFi).

Figure 2. Overall view experimental equipment and instruments for CFST.

The mix proportions of 01 cubic metre concrete are: PCB 40 Cement (Nghi Son, Vietnam): 395 kilograms; water: 210 litres; river sand: 530 kilograms; coarse aggregate: 1150 kilograms. The concrete strength B25 with slump of 12 centimeters follows to TCVN 5574:2012, [13], equal to C20/25 according to Eurocode 2 (EC2), [11] which is compressive strength for cylindrical concrete specimens $f_{c,cyl}$ of 20 MPa and modulus of elasticity of concrete E_c of 29×10^3 MPa at 28 days. Material properties of steel follow to BS 1387/1985, ASTM A53 with specified minimum yield stress F_y of 240 MPa and modulus of elasticity of steel E_s of 2×10^5 MPa. Three CFST specimens are shown in Figure 3. It is assumed that there is sufficient interaction between the steel pipe and the concrete core, then the ultimate bearing strength of CFST, $P_{u,cal}$ is determined according to Eurocode 4 (EC4) as follows, [12]:

$$P_{u,cal} = P_{a,cal} + P_{c,cal} = f_y A_a + f_{c,cyl} A_c \quad (1)$$

where: $P_{a,cal}$ is the nominal yielding strength of steel material; $P_{c,cal}$ is the nominal yielding strength of concrete material; f_y is specified minimum steel yield stress; $f_{c,cyl}$ is compressive strength for cylindrical concrete specimens; and A_a , A_c is are cross-sectional areas of the steel pipe and concrete core, respectively.

AISC 360-10: The specimens are classified as compact sections for filled composite sections subjected to axial compression, Width (D) to Thickness (t) Ratio is checked as follows, (Table II.1A – ANSI/AISC 360-10 Pages 16.1-84), [14]:

$$(D/t) < \lambda_p = (0.15 \times E_s) / F_y \quad (2)$$

The available compressive strength of axially loaded doubly symmetric filled composite members for compact sections shall be taken as, [14]:

$$P_p = F_y A_s + C_2 f'_c (A_c + A_{sr} \times E_s / E_c) \quad (3)$$

In which: coefficient of C_2 is 0.85 for rectangular sections and C_2 is 0.95 for round sections; A_{sr} is equal to 0.0 with no steel reinforcement (rebar) in composite members; F_y is specified minimum yield stress of steel section; A_s is area of steel; A_c is area of the concrete section; f'_c is specified compressive strength of concrete.

The mounting of the test specimen and the arrangement of Spring Return Linear Variable Differential Transformer (LVDT), strain gages are shown in Figure 4 and more clearly in Figure 5. The loading apparatus consists of compression testing machine pressure machine set with 100 tons, Model: WE-1000B produced by Wuxi Xiyi - China; LoadCell with 120000 lbs of RDP Electronics Ltd, UK (Model: RSL0710/120000LB) is used to measure compression force signal and installed at bottom of CFST. Strain gauge PL-60-11 (TML Tokyo Sokki Kenkyujo co., Ltd. - Japan) in concrete core is 60 mm length, 120 Ω gauge resistance, 2.13 gauge factor. Strain gauge PLA-5-11 (TML Tokyo Sokki Kenkyujo co., Ltd. - Japan) on steel surface is 5 mm length, 120 Ω gauge resistance, 2.13 gauge factor.



Figure 3. Manufacturing of CFST specimens.



Figure 4. Test setup for CFST column.

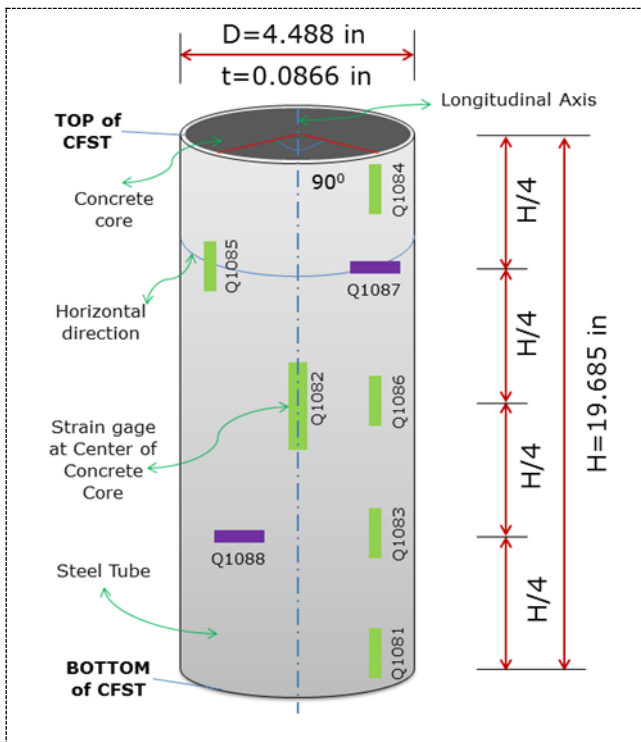


Figure 5. Schematic diagram of positions and identifications for strain gages.



Figure 6. Buckling failure mode of the steel tube surface.

The numerical results in CAE are shown in Figure 7 for observing and predicting failure mode of modelling CFST, and large deformation under compressive stresses on the steel tube’s surface near the concrete top surface also is described in this Figure. However, Three test specimens have different failure modes compared with numerical simulation of CFST model under axial load. Specimens, namely MUCE-01 is Euler buckling [15]; MUCE-02 is local buckling near the column top; The clearest result is MUCE-03 with outward local buckling in the region near the top and middle of CFST column, are shown in Figure 8.a, 8.b, 8.c respectively.

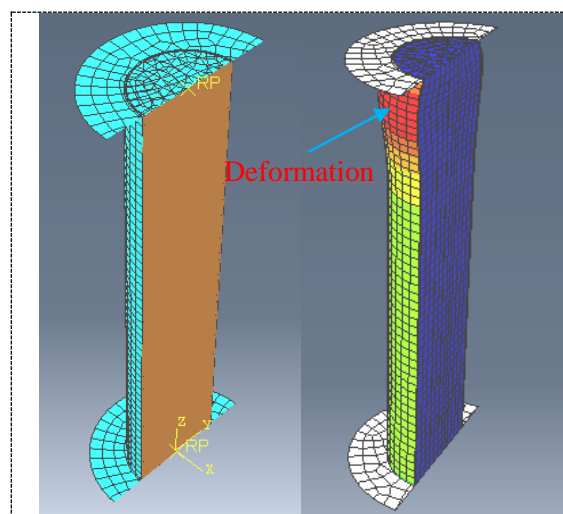


Figure 7. Finite element modelling of CFST column: steel tube and concrete core.



Figure 8. Tested results and failure modes of three CFST specimens.

Figure 9 illustrates the behavior of CFST specimen (MUCE-03) subjected to compression force. Figure 9.b shows force versus strain of strain gages at the top (Q1084), the bottom (Q1081), the middle (Q1086), H/4 (Q1085 and Q1083) of steel tube surface parallel to the longitudinal direction. It can be seen that loading is about 101100 lbf, compression strain at position H/4 (Q1085) decreases rapidly from 0.1104 to 0.05, part of the explanation lies in local outward buckling. Two strain gages including Q1087 and Q1088 are mounted at H/4 of steel surface in the horizontal direction for monitoring local buckling as shown in Figure 9.c. The axial load versus displacement (LV3552) with approximately maximum values: 116600 lbf and 1.119 inches in the Figure 9.d. Moreover, Figure 9.a demonstrates crack occurring in concrete core (installed strain gage - Q1082) due to local buckling, signal curve of Q1082 is interrupted, as well as some other signals can be errors at this time.

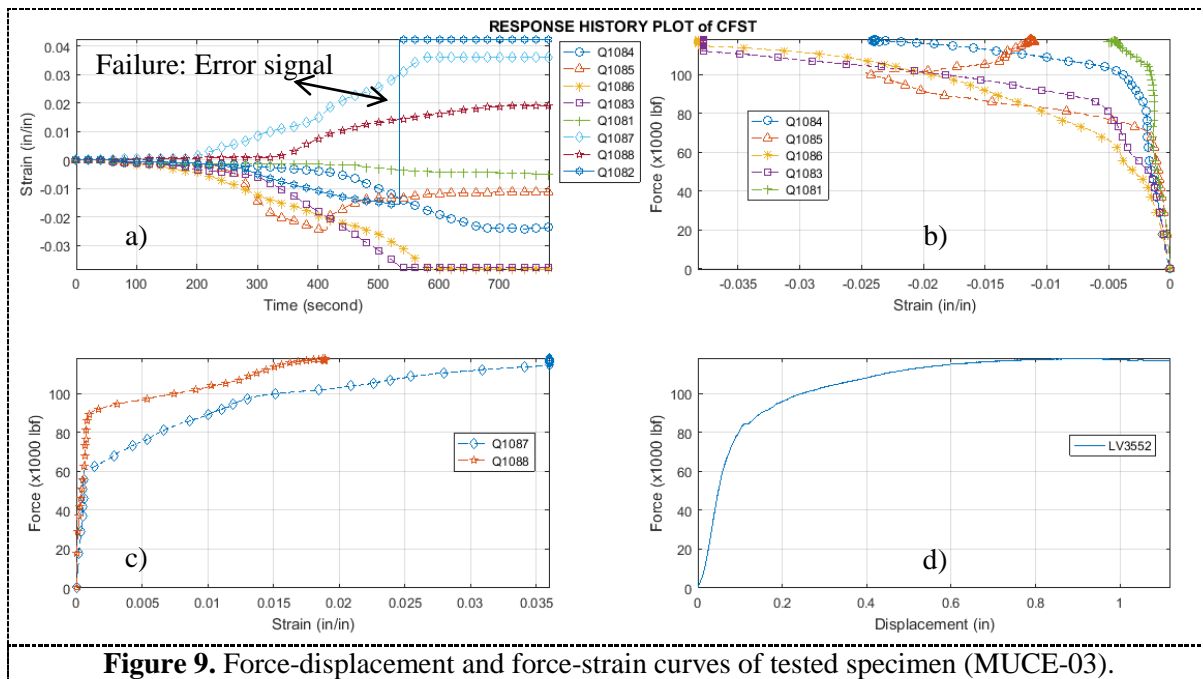


Figure 9. Force-displacement and force-strain curves of tested specimen (MUCE-03).

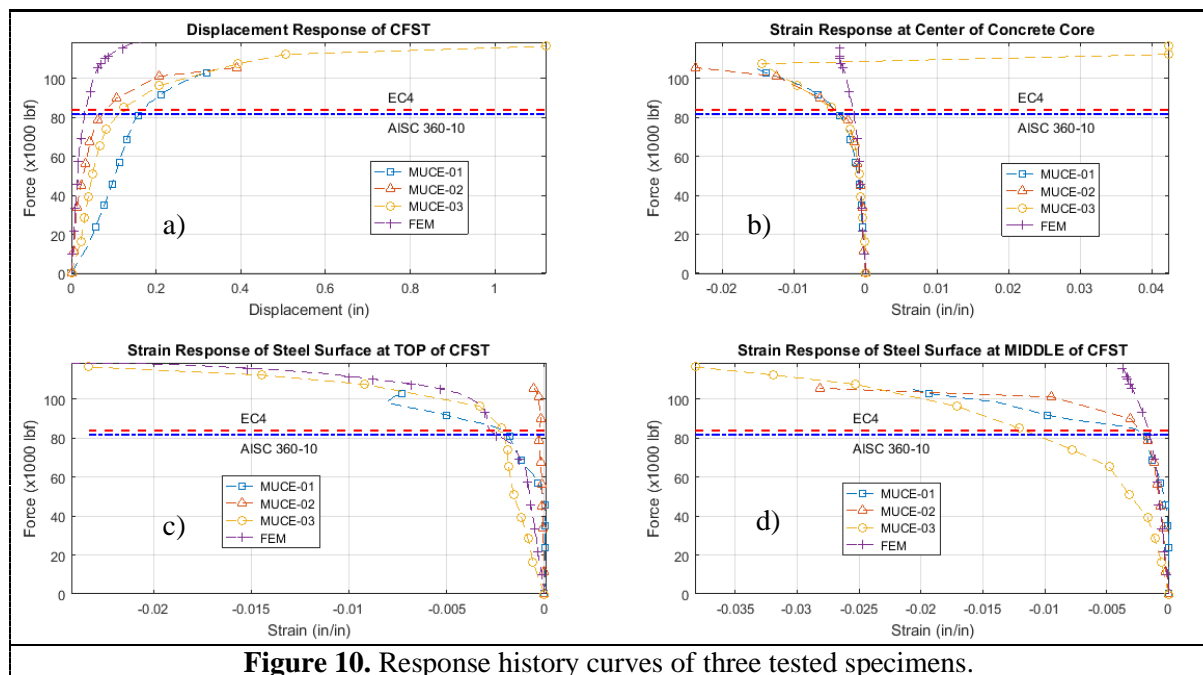


Figure 10. Response history curves of three tested specimens.

As shown in Figure 10 above and Figure 11 below, displacement and strain versus axial force graphs are measured in different positions of three specimens. As can be seen, MUCE-01, MUCE-02, MUCE-03 correspond to dashed line with square markers, dashed line with upward-pointing triangle markers, dashed line with circle markers, respectively. Load test records are compared with data in CAE for fracture simulation of CFST model applied to longitudinal compression and CAE result is dashed line with plus-sign markers. In this paper, ultimate strength of concrete-filled composite steel column is calculated by equation (1) according to EC4 with dashed line of this figure. Moreover, the ultimate capacity prediction of CFST is based on AISC 360-10 from the equation (3) with dash-dot line under line of EC4. According to EC4 and AISC 360-10 standard are about 84190,949 lbf (374.5 kN), 82504.882 lbf (365 kN), respectively, while the real axial load capacity of CFST specimen is approximately equal to 96430 lbf (nearly 429 kN) under failure modes higher than design standards. From Figure 10.a, it is observed that critical load of CFST specimens reaches a peak at just over 101200 lbf (450 kN) and then loading increases very slowly while strain signal is error in Figure 10.b, partly because of failure criterion for concrete core, partly because local buckling occurs in the region near the top of column in Figure 10.c and the region near the mid-height of specimen in Figure 10.d. Strain values in CAE modelling are less than results in experiment of figures because CFST modelling is not calibrated, steel and concrete's modulus of elasticity can be changed to compare with design standards. From CAE modelling of CFST can be used to simulate failure modes, and then support in planning and optimisation for installing sensors, and can be used to calculate ultimate strength calculations of CFST column under axial compression.

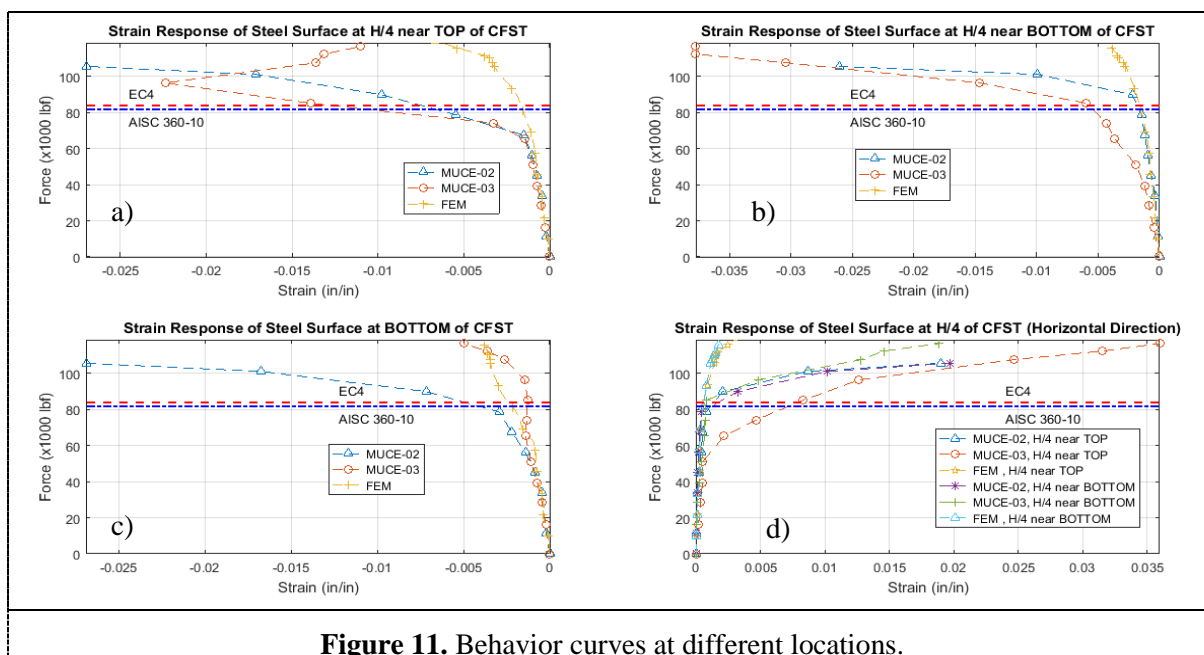


Figure 11. Behavior curves at different locations.

In Figure 11.a, strain data at region of H/4 rises significantly (MUCE-02), MUCE-03 jumps sharply then goes down moderately. This means that, large deformation on steel surface corresponding to region of local buckling is unstable (Figure 11.b, c, d). Buckling modes can be monitored by strain gages at weak locations near top and bottom of CFST column.

3. Conclusions

The following principal conclusions are drawn from the results that were obtained in the study:

- The ultimate strength of CFST specimen under axial load was determined by EC4, AISC 360-10 and strain measurement.
- The location of local buckling failure of CFST column was observed clearly through testing procedure, and also showed in CAE modelling. Comparison between measured results and predicted by uncalibrated model was moderately error because material properties, friction coefficients of steel and concrete were obtained as described in design standards and studied papers. In order to solve

limitations of this paper, the modelling of CFST member can be updated by data of strain and force load overtime in the further work.

- The wireless structural testing system (STS-WiFi) in this study was correctly measured and recorded dynamic and static time historical responses of CFST specimens. This experimental equipment and instruments can be used in long-term structural health monitoring (SHM) for CFST members and other structures including: buildings, bridges, industrial structures based on Non-Destructive Testing-NDT in the field.

4. References

- [1] Manojkumar V. Chitawadagi, Mattur C. Narasimhana and M. Kulkarni 2010, Axial strength of circular concrete-filled steel tube columns - DOE approach, *Journal of Constructional Steel Researched* G. A. R. Parke (England: Elsevier) volume 66 issue 10 pp 1248-1260.
- [2] Y F Yang and L H Han 2012, Concrete filled steel tube (CFST) columns subjected to concentrically partial compression, *Thin-Walled Structures* ed N. Silvestre (Portugal: Elsevier) volume 50 issue 1 pp 147-156.
- [3] M. Dundu 2012, Compressive strength of circular concrete filled steel tube columns, *Thin-Walled Structures* ed N. Silvestre (Portugal: Elsevier) volume 56 pp 62-70.
- [4] Talha Ekmekyapar and Baraa J.M.AL-Eliwi 2016, Experimental behavior of circular concrete filled steel tube columns and design specifications, *Thin-Walled Structures* ed N. Silvestre (Portugal: Elsevier) volume 105 pp 220-230.
- [5] A. K. H. Kwan, C. X. Dong and J. C. M. Ho 2016, Axial and lateral stress–strain model for concrete-filled steel tubes, *Journal of Constructional Steel Researched* G.A.R. Parke (England: Elsevier) volume 122 pp 421-433.
- [6] C. X. Dong, A. K. H. Kwan and J. C. M. Ho 2017, Effects of external confinement on structural performance of concrete-filled steel tubes, *Journal of Constructional Steel Researched* G. A. R. Parke (England: Elsevier) volume 132 pp 72-82.
- [7] Y. Ouyang, A. K. H. Kwan, S. H. Lo and J. C. M. Ho 2017, Finite element analysis of concrete-filled steel tube (CFST) columns with circular sections under eccentric load, *Engineering Structures* ed P.L. Gould (USA: Elsevier) volume 148 pp 387-398.
- [8] Qing-Xin Ren, Lin-Hai Han, ChaoHou, Zhong Tao and ShuaiLi 2017, Concrete-encased CFST columns under combined compression and torsion: Experimental investigation, *Journal of Constructional Steel Research* ed G. A. R. Parke (England: Elsevier) volume 138 pp 729–741.
- [9] Liusheng He, Yangang Zhao and Siqi Lin 2017, Experimental study on axially compressed circular CFST columns with improved confinement effect, *Journal of Constructional Steel Research* ed G. A. R. Parke (England: Elsevier) volume 140 pp 74–81.
- [10] Fang Yuan, Mengcheng Chen, Hong Huang, Li Xie and Chao Wang 2017, Circular concrete filled steel tubular (CFST) columns under cyclic load and acid rain attack: Test simulation, *Thin-Walled Structures* ed N. Silvestre (Portugal: Elsevier) volume 122 pp 90–101.
- [11] Eurocode 2, 2004, Design of concrete structures, *European Committee for Standardization* EN1992-1-1.
- [12] Eurocode 4, 2004, Design of composite steel and concrete structures, part 1.1: General rules and rules for buildings, *European Committee for Standardization* EN1994-1-1.
- [13] TCVN 5574-2012, Concrete and reinforced concrete structures - Design standard, Vietnam.
- [14] Specification for Structural Steel Building 2010, American Institute of Steel Construction.
- [15] Timoshenko S. P. and Gere J. M. 1961. Theory of Elastic Stability, 2 ed., McGraw-Hill.
- [16] Amar Khennane 2013, Introduction to Finite Element Analysis Using MATLAB and Abaqus, *Taylor & Francis Group*, USA.
- [17] Bridge Diagnostics Inc 2015, Wireless Structural Testing System STS-WiFi Operations Manual (Colorado: USA).

Acknowledgments

The authors would like to thank the Mien Trung University of Civil Engineering (MUCE, LAS-XD 162) in Phu Yen province, Ministry of Construction of the Socialist Republic of Vietnam (MOC) for supporting this research project.